Pergamon
www.elsevier.com/locate/actaastro
Acta Astronautica Vol. 50, No. 7, pp. 433–443, 2002

PII: S0094-5765(01)00188-6
0094-5765/02/$ - see front matter

THE MICROSCOPE MISSION†

PIERRE TOUBOUL‡, BERNARD FOULON, and LAURENT LAFARGUE,
Physics & Instrumentation Departement, Office National d'Etudes et de Recherches Aérospatiales (ONERA), BP 72, 92322 Châtillon Cedex, France

and

GILLES METRIS
CERGA, Observatoire de la Côte d'Azur Av. Nicolas Copernic, 06310 Grasse, France

(Received 22 February 2001)

Abstract—The MICROSCOPE mission had been selected at the end of 1999 by the French space agency Cnes for a launch scheduled in 2004. The scientific objective of the mission is the test of the Equivalence Principle (EP) up to an accuracy of 10^{-15} with its well-known manifestation, the universality of free fall. This principle, at the origin of general relativity, is only consolidated by experimental results and presently with an accuracy of several 10^{-13}. The micro-satellite developed by Cnes weighs less than 120 kg and is compatible with a low-cost launch like ASAP ARIANE V. The instrument is composed of two differential electrostatic accelerometers operating at finely stabilised room temperature. Each accelerometer includes two cylindrical and concentric test masses, made of platinum or titanium alloys. The experiment consists in controlling the two masses in the same orbital motion. Because of the drag compensation system of the satellite including field effect electrical thrusters, this motion is quite purely gravitational. The electrostatic control forces used in the differential accelerometers are finely measured. The principle of the experiment is presented, the configuration of the instrument and of the satellite is detailed with regard to the present development status. The specifications for the major parameters of the experiment are detailed.

1. MISSION OVERVIEW

The MICROSCOPE mission, French acronyms for MICROSatellite with drag Control for the Observation of the Equivalence Principle (EP), has been proposed and studied during the last two years by the Onera and Cerga Institutes before being recently selected by the French space agency Cnes. This mission exploits the micro-satellite product line, the satellite mass being less than 120 kg and compatible with a low-cost launch like ASAP ARIANE V.

The scientific objective of the mission is the test of the EP with an accuracy of 10^{-15} i.e. about three orders of magnitude better than the accuracy of the present on ground experiments. All recent laboratory experiments exploit torsion pendulum and have to deal with the environmental instabilities and in particular the Earth gravity gradient fluctuations [1–3]. Recent results have been obtained by considering the Earth–Moon laser ranging data but the material composition of the two celestial bodies is not very well identified [4] to interpret the results. Such an improvement in confirming the equivalence between inertial mass and gravitational mass represents an important verification of the relativist theory of gravitation and other metric theories, which postulate this principle and should emphasise the interest of more accurate experimental or observational data on the post Newtonian coefficients [5,6]. The violation of the EP that is an exact symmetry for general relativity would open the way to the demonstration of a new interaction that is expected by many quantum theories of gravity in progress [7–9].

†Paper IAF-00.J.1.06 presented at the 51st International Astronautical Congress, Rio de Janiero, Brazil, Oct. 2–6, 2000.
‡Corresponding author. Tel.: +33-1-4673-4832; fax: +33-1-4673-4148.
E-mail address: touboul@onera.fr (P. Touboul).

Approaches to quantum theory like Superstring theory are presently of intense activities and the existence of extra massless scalar field that naturally violate the EP needs to be lightened by experimental data like EP test results, the most sensitive low-energy probes. The non-violation with a better accuracy than obtained now would be a stronger constraint for great unification theories. MICROSCOPE will then be the first space attempt for the search of direct evidence of new gravitational phenomena before even more ambitious missions with better accuracy [10–12].

MICROSCOPE experiment exploits the Earth as the gravitational source. The in orbit motion of two masses falling in the Earth's gravity field and composed of two different materials is controlled to be identical, taking care that both masses are submitted exactly to the same gravitational field. The fine observation of the only force added to break the experimentation symmetry would provide the expected test results. This experimentation shall take advantage of the very soft environment provided on board a drag-free satellite, the non-gravitational force applied on the satellite being compensated by the actuation of electrical thrusters: definitively less gravity gradient fluctuations and no human activity perturbations. The possibility of a very long time of observation of the free fall mass motion in steady conditions leads to expected signal integration over days to the benefit of the rejection of stochastic disturbances. The rotation of the observational frame with respect to the gravity field orientation also helps in the discrimination of the eventual EP violation signal; moreover, several rotation frequencies can be considered. Then the EP test is performed at orbital or several orbital frequencies, the stability of 1% rotation rate is required in agreement to filtering bandwidth.

The satellite payload is composed of two quite identical accelerometers. Each differential accelerometer includes two cylindrical and concentric test masses. The masses are made of the same material for the first one which is dedicated to assess the accuracy of the EP experimentation. The mass materials are different for the second one. Then, the experimentation procedure is based on a double comparison in order to suppress the systematic errors. The selection of the mass material is a compromise between the instrument accuracy requirements and the theoretical interest. The ability of micrometric geometry achievement, the thermal stability and ageing, its magnetic susceptibility and surface electrical property, its off-gazing and chemical stability are properties to be considered as well as difference of nuclei components related to new possible interaction [9] or to already performed EP tests [3]. Platinum is presently selected for three of the masses and titanium for the last one. The weight of the masses ranges from 0.4 up to 1.7 kg. Couple of more masses and materials are obviously of great interest but not compatible with the micro-satellite power and mass availability; the success of the mission will certainly open the door to further missions.

The test-mass motions, with respect to highly stable silica instrument frame, are servo-controlled by using very accurate capacitive position sensing and electrostatic actuators. The relative position of the two masses is thus maintained motionless with a 2×10^{-11} m/$\sqrt{\text{Hz}}$ stability and the fine comparison of the electrostatic control force with a better resolution than 5×10^{-13} N/$\sqrt{\text{Hz}}$ leads to the EP test with the expected 10^{-15} accuracy with an integrating period of about one day.

The attitude as well as the atmospheric and thermal drag of the satellite are actively controlled in such a way that the satellite follows the two test masses in their gravitational motion, thanks to the specific drag compensation and attitude control system. The mission duration is one year, most of this time being dedicated to the instrument calibration and to the determination of the instrument sensitivity to the external environment disturbances like gravity gradients for instance.

The satellite drag compensation involves field emission electric propulsion (FEEP) [13,14] and in addition to the measurement mode when the satellite shields the instrument from Earth's and Solar radiation pressure and from atmospheric drag, this system allows a fine calibration of the instrument by generating well-known cinematic accelerations in all six degrees of freedom.

2. THE MICROSCOPE PAYLOAD

2.1. Electrostatic differential accelerometers

The scientific instrument dedicated to this mission is derived from the space ultrasensitive accelerometers already developed by the authors in view of Earth's gravity field global and fine recovery. These tri-axial electrostatic accelerometers which have been designed and tested for the CHAMP [15,16] and GRACE [17] missions are being developed now for the GOCE mission [18,19]. The instrument comprises two similar differential accelerometers.

Each differential accelerometer is composed of two concentric electrostatic accelerometers (see Fig. 1 and Fig. 2). The test mass of each accelerometer is maintained along the three directions at

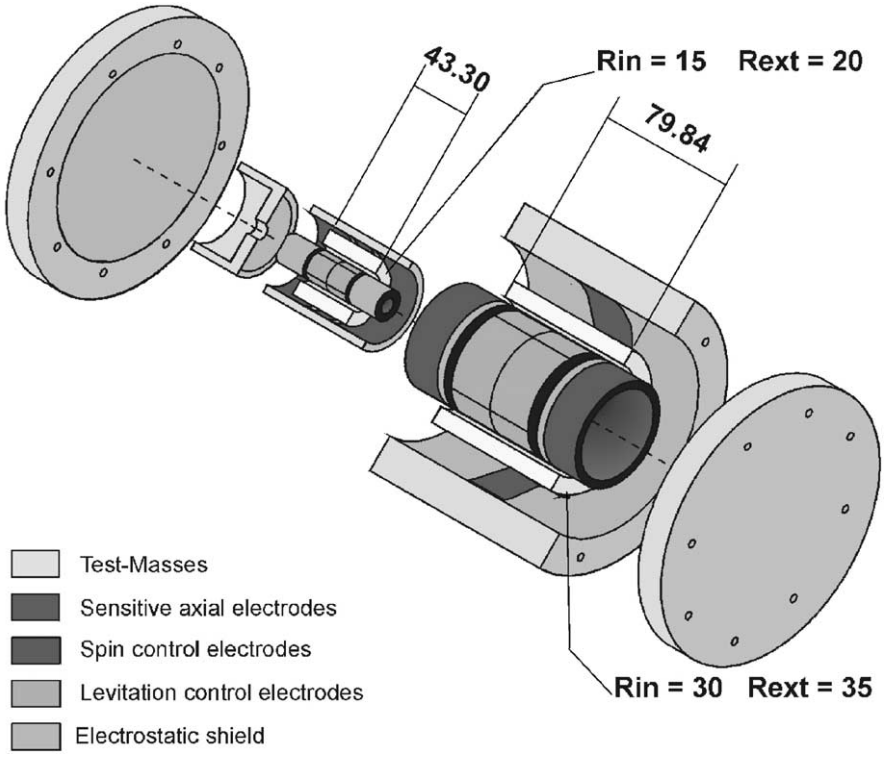

Fig. 1. Differential accelerometer sketch.

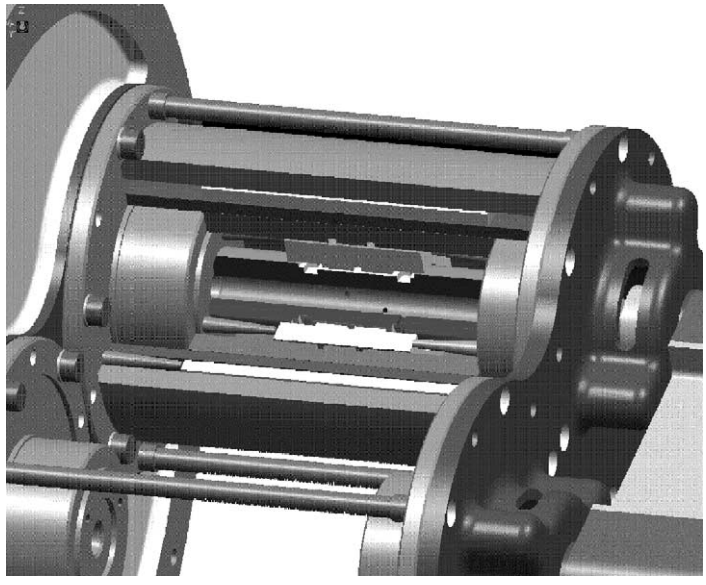

Fig. 2. Differential accelerometer CAD drawing.

the centre of the fused silica instrument cage by electrostatic forces. Electrodes are engraved in the metallic coating deposited on the cage all around the mass. These electrodes are used for the capacitive sensing of the mass position and attitude. From these sensing data, dedicated set of voltages are computed and applied on the same electrodes to servo-control the mass motionless. The accurate measurement of these voltages leads to the resultant of the generated electrostatic forces. Both masses are then controlled with respect to the same silica frame: the sum of these forces is maintained null by the satellite drag compensation system that acts on the thrusters to move the instrument silica

frame following the masses; the difference of the electrostatic forces is then observed along the orbit to the search of the EP violating signal.

The cylindrical test masses present sphere-like inertia matrices to limit the effects of the satellite and the Earth gravity gradients. The electrode configuration presented in Fig. 2 allows the measurement and the control of the six degrees of freedom of each test-mass. While the eight quadrant electrodes associated by pairs allow the control of the radial translations and rotations, the two cylindrical sensing electrodes at the ends of the test-masses are used to control motionless the test-masses along the axial direction. This electrode configuration is optimised along the axial direction in view of reducing the back action on the mass motion from the electrical signals for capacitive sensing and in view of reducing the electrostatic stiffness and damping between the mass and the instrument frame for a range of mass position along this axis.

The cylindrical test masses are centred during the instrument integration with an accuracy of 10 μm. The relative position of the two masses will be evaluated in orbit through ground data processing. An accuracy of 0.1 μm is expected by exploiting the differential effect on the masses of the Earth's gravity gradient field. The relative position of the masses can be modified by offsetting the electrostatic servo loops: verification of the instrument sensitivity to this parameter will be performed during the calibration phase as well as rejection rate of the Earth's gravity gradient signal.

In the useful difference signal of the experiment, the common acceleration of the masses is rejected and in particular the residual cinematic acceleration of the satellite that is not compensated by the gravity field. This is true when the sensitivity and the orientation of the two accelerometers are matched. This will be done during the calibration phase by shaking the satellite with the propulsion system at well-known frequency along the three axes. A matching of 100 part per million is expected that is coherent with the $10^{-9}\ \mathrm{ms}^{-2}\ \mathrm{Hz}^{1/2}$ level of the expected residual satellite drag.

The resolution of this instrument has been evaluated from the noise of the electronics circuits, as measured in the laboratory, from the mass motion sources of disturbance, as modelled after experimental investigations and from the environment sensitivity. A $10^{-12}\ \mathrm{ms}^{-2}\ \mathrm{Hz}^{1/2}$ resolution is attained at frequencies around 10^{-3} Hz, i.e. several orbital frequencies corresponding to the instrument frame angular rate with respect to the Earth's pointing frame.

As summarised in Fig. 3, at lower frequencies, the thermal instabilities ΔT induce radiation pressure and radiometer acceleration fluctuations due to the residual gas at pressure P for the latter:

$$\Gamma_{\mathrm{radiometer}} \approx \frac{1}{2m} PS \frac{\Delta T}{T},$$

where m is the mass of the test-mass and S is the area considered in the direction of the thermal gradient.

At higher frequencies, the position sensing resolution affects the resolution with a square frequency law.

$$\Gamma_{\mathrm{posnoise}} = x_{\mathrm{noise}}(\omega^2 + \omega_p^2).$$

The selected configuration leads to computed passive stiffness (different from the active servo-loop one) between the mass and the instrument frame of less than 5×10^{-3} N/m ($\omega_p < 0.1$ rad/s) and so negligible effects at lower frequencies.

The thermal noise of the mass motion is derived from the damping factor estimated from dedicated laboratory experiments [20,21] and mainly due to the thin 5 μm wire used for the charge control of the mass.

$$\Gamma_{\mathrm{wire}} = \frac{1}{m}\sqrt{4k_b T H_{\mathrm{wire}}},$$

where H_{wire} represents the gold wire damping.

2.2. *Instrument configuration on board the satellite*

Both differential accelerometer cores are integrated in tight vacuum housings that also provide thermal insulation and magnetic shielding: fluctuations of the instrument temperature shall be less than half a degree over one orbit. These housings are mounted near the satellite centre of mass in order to reduce the torque demanded by the propulsion systems to maintain the satellite rotation but no more stringent requirement is considered: the satellite drag compensation is performed thanks to the accelerometer outputs in order to nullify the mass common disturbance whatever the satellite centre of mass motion around them is. The accelerometer sensitive axes are oriented in the orbital plane along the spacecraft X-axis, the centres of the test masses being on the rotating axis of the satellite, normal to the orbital plane. The total mass of the payload is estimated to less than 25 kg (see Table 1) compatible with Cnes micro-satellite design and launch opportunities.

The instrument electrical power has been estimated according to the different envisaged phases of operation during the mission, leading to about 13 W on the non-regulated 28 V satellite power bus

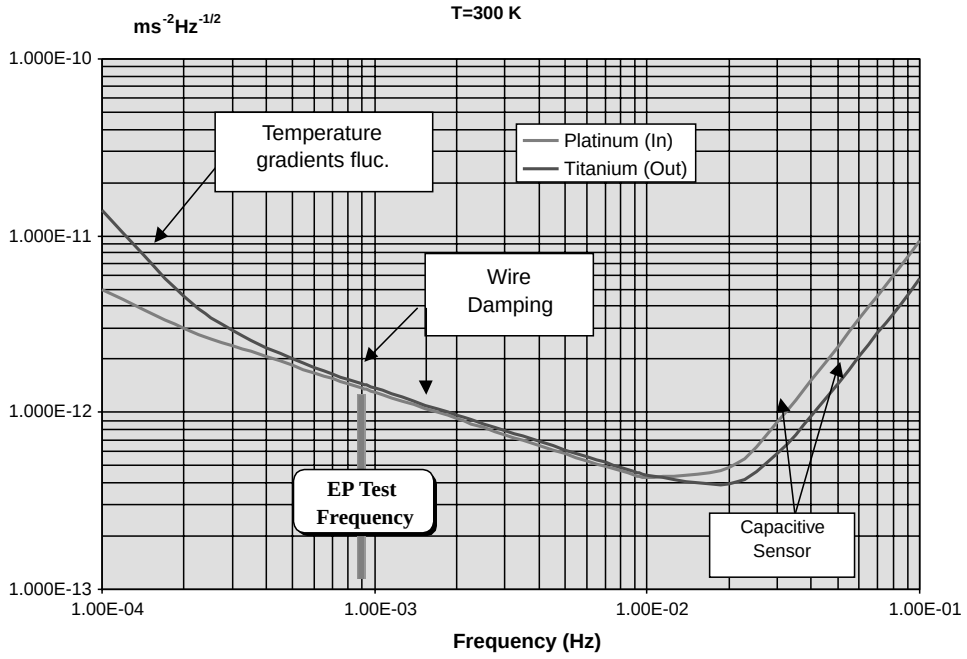

Fig. 3. Accelerometers error budget.

Table 1. Instrument mass and volume

Accelerometer	Mass (kg)	Volume (mm^3)
Mechanics		
Acc1 (Pt-Pt)	2.5	
Acc2 (Pt-Ti)	2.0	
Blocking actuators	0.5	
Housing & mechanical interfaces	6.0	$250 \times \varnothing 200$
Electrical interfaces	1.5	
Electronics		
Analog	4.5	$4 \times (150 \times 180 \times 120)$
Digital	6.0	$4 \times (120 \times 180 \times 180)$
Margin (10%)	2.5	
Total	25	

with only one differential accelerometer operating and 25 W when both are switched on.

3. MICROSCOPE SATELLITE

3.1. Satellite configuration

The present opportunity of launch is Ariane V as a complementary passenger of the French HELIOS 2 main satellite scheduled at the beginning of 2004. The heliosynchronous quasi-circular injection orbit at the altitude near 700 km is much more favourable for the mission. The in orbit configuration of the satellite is presented in Fig. 4.

The satellite is rather compact with no deployable solar panel to ensure a high rigidity: any mass

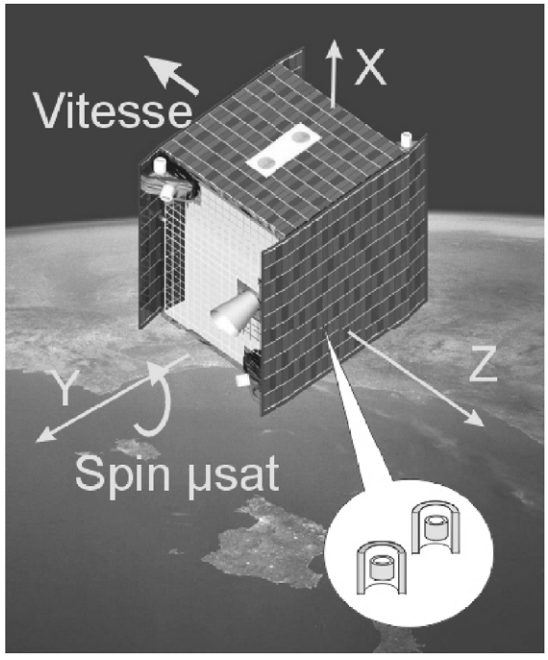

Fig. 4. The MICROSCOPE satellite, configuration orbit (courtesy *Cnes*).

motion on board is avoided and no momentum wheel is used during the experimental operation. Attention is paid to the thermo-elastic behaviour of the satellite, the structure of which is realised with aluminium honeycomb and plates. The three solar panels will be mounted on three faces of the bus. High efficiency AsGa solar cells will be used in

Table 2. Thermal environment specifications

	Electronics unit	Mechanics unit
Operating temperature	$+10^{\circ}$C to $+50^{\circ}$C	$+20^{\circ}$C to $+40^{\circ}$C
Thermal variations		
Random (about f_{EP})	5 K/Hz$^{1/2}$	5 K/Hz$^{1/2}$
Nodal (at f_{EP})	sinus 0.01 K	sinus 0.01 K
Thermal Gradients		
Random (about f_{EP})	No	1 K/(m Hz$^{1/2}$)
Nodal (sinus at f_{EP})	No	0.001 K/m

Table 3. Main specifications for the DAOCS (Y & Z the less sensitive axes for the instrument)

	About Y, Z or along Y, Z	
	Max. value at DC	Stability at f_{ep}
Ω angular velocity	10^{-5} rad/s	10^{-5} rad s^{-1} Hz$^{-1/2}$
dΩ/dt angular acc.	10^{-5} rad s^{-2}	3×10^{-8} rad s^{-2} Hz$^{-1/2}$
Γ linear acc.	3×10^{-9} m s^{-2}	10^{-9} m s^{-2} Hz$^{-1/2}$

Table 4. Main specifications for the DAOCS (X is the most sensitive axis for the instrument)

	About X or along X	
	Max. value at DC	Stability at f_{ep}
Ω angular velocity	10^{-5} rad/s or 2×10^{-3} rad/s (spin)	10^{-5} rad s^{-1} Hz$^{-1/2}$
dΩ/dt angular acc.	10^{-5} rad s^{-2}	10^{-7} rad s^{-2} Hz$^{-1/2}$
Γ linear acc.	3×10^{-9} m s^{-2}	10^{-9} m s^{-2} Hz$^{-1/2}$

Table 5. Accelerometers full range

Accelerometer axes	Safe mode
X (axial)	5×10^{-6} m s^{-2}
Y and Z (radial)	5×10^{-5} m s^{-2}
Rotation about X	10^{-5} rad s^{-2}
Rotation about Y or Z	10^{-4} rad s^{-2}
Accelerometer axes	**Measurement mode**
X (axial)	10^{-7} m s^{-2}
Y and Z (radial)	5×10^{-6} m s^{-2}
Rotation about X	10^{-6} rad s^{-2}
Rotation about Y or Z	10^{-5} rad s^{-2}

order to obtain available power of 80 W, equally shared for the payload, the electrical propulsion and the satellite module. Moreover, to limit magnetic disturbances due to test-mass susceptibility, the magnetic moments on board the satellite shall be limited and steady, variations less than 0.1 Am^2 in the EP frequency vicinity and at 30 cm from the instrument are specified. This concerns particularly the magneto-torquers or the batteries. Thermal stability of the apparatus is required and according to the developed thermal model, the following stabilities must be considered (see Table 2).

3.2. *Satellite attitude*

During the mission, the satellite is Earth pointing, inertial pointing or rotating about the Y-axis, normal to the orbital plane with rather low angular rates about 2×10^{-3} rad/s. The frequency f_{EP} at which the experiment is realised is then the sum of the orbital frequency and the spin frequency. The normal plane to the satellite axis of rotation, the orbital plane and the accelerometer sensitive axes have to be aligned with a better accuracy than 10^{-2} rad requiring alignment of the star tracker with respect to the instrument (see following chapter).

Detailed specifications concerning the satellite motion and the attitude variations are shown in Tables 3 and 4. These specifications have been deduced by expressing the motions of the masses in the satellite reference frame and by considering the defects of symmetry of the instrument. The drag, attitude and orbit control system (DAOCS) shall meet these requirements by taking advantage of the accelerometer outputs (linear but also angular accelerations). Four pods of two or three electric thrusters are installed on the corners of two opposite faces, one of them containing the star tracker with its baffle and the satellite radiator: the configuration is optimised for torque control, 12 thrusters allowing redundancy. Each thruster can enable a maximum thrust of 50–100 μN with a quantification step of 0.1 μN.

Besides these performance specifications, it is also important to ensure the instrument operation in safe mode or when the drag compensation and the fine attitude control is not operating with the instrument data. Then, the full range of operation of the accelerometers have to be considered as in Table 5.

These ranges also have to be considered when both differential accelerometers are operating: the drag-free point at the centre of one accelerometer leads to a centrifugal acceleration applied on the second one when the satellite rotates; fortunately, the rotation axis is crossing the two accelerometer centres to the defect of the instrument and the satellite geometry.

3.3. *Mission operation*

The mission duration of one year is subdivided into six phases. After the heliosynchronous orbit

injection, the satellite is controlled in safe mode, Earth pointing, with the nominal equipment of the microsatellite platform: sun sensor and star tracker, magnetotorquers and reaction wheels. In the second phase, the two differential accelerometers are switched on, one by one and their operations are verified, as well as the electrical propulsion is calibrated. Then the drag-free and the fine attitude control is switched on and verified. In the fourth phase, the accelerometers are switched in their mode of highest sensibility and the instrument and the DAOCS is accurately characterised: residual acceleration levels, stability of rotation axis and frequency, coupling between axes, instrument sensitivity to environment and gravity gradients. After all calibrations, the EP experiment is realised with the first differential accelerometer in inertial and spinning attitudes, and with two angular phases along the orbit (defined at the equator passage). In order to verify that no severe drifts have occurred between the beginning and the end of the experiment, the previous phase of calibration is performed again. The EP experiment is then performed with the second differential accelerometer with a new calibration at the end. According to the integration periods required for the filtering of the data, the minimum duration is estimated to be 6 months. The extra time will be used to assess the experiment and to perform complementary operations like:

- the drag-free system operation with a control versus the test mass relative position to the satellite, like in the LISA future space mission dedicated to the observation of gravity waves [22], instead of a control versus the acceleration provided by the instrument like in MICROSCOPE baseline operation;
- the gravity gradiometer operation and calibration by exploiting two single accelerometers of different housing, then not concentric, like in the GOCE mission [18,19];
- the FEEP's neutralisation efficiency,
- the ground laser tracking of the micro-satellite,
- the altitude decrease, the aerology analysis and the atmosphere entry methodology, etc.

The scientific mission centre will be located in Onera premises and will be in charge of sending the telecommands through the Control Centre in Cnes, to pre-process and to archive the scientific and housekeeping data, to partially process the measurements for quasi-real-time overview of the experiment and to manage the exchanges between Onera and Cerga for the fine analysis. The total data flow rate is evaluated to be 1008 bits/s, so less than 90 Mbits per day. The satellite memory of 1 Gbits capacity and the rate of the TM/TC link to the ground station of 400 kbits/s is compatible with the payload needs.

4. ORBIT AND ATTITUDE SPECIFICATIONS

Besides the instrument design and accommodation on board the satellite, fine software simulations try to analyse in details the experimental procedures and the assumed data process.

4.1. The main signal

To derive the main specifications for orbit and attitude by a straightforward analysis, we shall make use of a simplified model for the measured signal; the measured differential acceleration between two test-masses of centre of mass $\mathbf{C}'$ and $\mathbf{C}''$ is expressed as

$$\boldsymbol{\Gamma} = \boldsymbol{\Gamma}' - \boldsymbol{\Gamma}'' = (\delta'' - \delta')\mathbf{g} + [\mathbf{T}]\mathbf{C}'\mathbf{C}'' - [\mathbf{I}]\mathbf{M}'\mathbf{M}''. \quad (1)$$

- The first term of the RHS represents a signal of violation of the universality of free fall which is to be detected: $\delta = m_g/m_i$ where m_g and m_i are the gravitational and inertial masses, respectively, and $\mathbf{g}$ is the gravity acceleration in the neighbourhood of the test-masses.
- The second term reflects the effect of the spatial variations of the gravity: $[\mathbf{T}]$ is the gravity gradient tensor, i.e. the second order derivative matrix of the gravity potential.
- The third term represents the inertial acceleration due to the rotation of the accelerometer cages: $[\mathbf{I}]$ is the tensor of inertia which is significant only if the satellite is spined and $\mathbf{M}'$ and $\mathbf{M}''$ are the points of the cages from which the motions of $\mathbf{C}'$ and $\mathbf{C}''$ are detected.

The orders of magnitude are the following:

- from previous experiments on ground[3], $\delta'' - \delta'$ is smaller than 10^{-12} for some materials and the objective of the MICROSCOPE mission is to measure this quantity with an accuracy of 10^{-15} (hence a relative accuracy of 10^{-3} is needed).
- For a rather low orbit which is expected for MICROSCOPE, $\mathbf{g}$ has a magnitude standing between 5 and 8 m s^{-2} and the components of the gravity gradient tensor have magnitudes of about 10^{-6} s^{-2}.

- The spin rate of the satellite approaches a few 10^{-3} rad s^{-1} to optimise the accelerometer response, resulting in inertial terms of about 10^{-5} s^{-2} (in case of spin).

As the off-centring $\mathbf{C}'\mathbf{C}''$ and $\mathbf{M}'\mathbf{M}''$ should be of about 10^{-5} m by construction, we conclude that the objective is to detect an EP signal of a few 10^{-15} m s^{-2} in a signal dominated by the gravity gradient contribution of a few 10^{-11} m s^{-2} and by the inertial acceleration of a few 10^{-10} m s^{-2}. Hopefully, as we will show in the following, the different contributions have very different temporal spectra.

For a first analysis, only the main term (the monopolar term) of the Earth's gravity will be considered: the quadripolar contribution which is three orders of magnitude smaller and the other spherical harmonics will be neglected here. With this assumption, the components of **g** and [**T**] in an Earth's fixed frame are:

$$g_i = -\frac{\mu}{r^2}\frac{x_i}{r}, \tag{2}$$

$$T_{ij} = -\frac{\mu}{r^3}\left[\delta_{ij} - 3\frac{x_i}{r}\frac{x_j}{r}\right], \tag{3}$$

where $\mu \approx 4 \times 10^{-14}$ m^3 kg^{-1} s^{-2} is the Earth's gravitational constant, x_i are the rectangular co-ordinates of the current point in Earth's fixed orthonormal frame and $r = (x_1^2 + x_2^2 + x_3^2)^{1/2}$ is the distance to the geocentre; δ_{ij} is the Kronecker symbol.

With the monopole approximation, these expressions remain the same in other frames deduced from the Earth's fixed frame by rotation. We will use the orthonormal nodal frame $[\mathbf{h}, \mathbf{k}, \mathbf{w}]$ with **h** along the ascending node of the orbit, **w** along the angular momentum of the satellite (normal to the orbital plane. This frame is quasi-inertial (it undergoes only the slow rotation of the node) and allows to highlight the temporal variations of the satellite coordinates:

$$\begin{aligned}
\frac{x_1}{r} &= \cos(f+\omega) \\
&= \cos\lambda + e\cos(2\lambda-\omega) - e\cos\omega + O(e^2), \\
\frac{x_2}{r} &= \sin(f+\omega) \\
&= \sin\lambda + e\sin(2\lambda-\omega) - e\sin\omega + O(e^2), \\
\frac{x_3}{r} &= 0, \\
\frac{r}{a} &= 1 - e\cos f + O(e^2) \\
&= 1 - e\cos(\lambda-\omega) + O(e^2),
\end{aligned} \tag{4}$$

where f is the true anomaly of the satellite, a, e and ω are the semi-major axis, the eccentricity and the argument of the perigee of its orbit, respectively, and $\lambda = M + \omega$ (M is the mean anomaly) is the mean argument of the latitude. λ is a fast angle which has a frequency $\Lambda \approx n = (\mu/a^3)^{1/2}$ whereas ω has a low frequency (about 10^3 smaller than Λ).

Substituting eqn (4) into (2) and (3), we get the following expressions for the components, in the nodal frame, of the gravity acceleration vector and of the gravity gradient tensor:

$$\begin{aligned}
g_1 &= -\frac{\mu}{a^2}[\cos\lambda + 2e\cos(2\lambda-\omega)] + O(e^2), \\
g_2 &= -\frac{\mu}{a^2}[\sin\lambda + 2e\sin(2\lambda-\omega)] + O(e^2), \\
g_3 &= 0,
\end{aligned} \tag{5}$$

$$\begin{aligned}
T_{11} &= \frac{1}{2}\frac{\mu}{a^3}\left[1 + 3\cos(2\lambda) + e\left(-\frac{3}{2}\cos(\lambda+\omega)\right.\right. \\
&\quad \left.\left. + 3\cos(\lambda-\omega) + \frac{21}{2}\cos(3\lambda-\omega)\right)\right] \\
&\quad + O(e^2), \\
T_{12} &= \frac{1}{2}\frac{\mu}{a^3}\left[3\sin(2\lambda) + e\left(-\frac{3}{2}\sin(\lambda+\omega)\right.\right. \\
&\quad \left.\left. + \frac{21}{2}\sin(3\lambda-\omega)\right)\right] + O(e^2), \\
T_{13} &= 0, \\
T_{22} &= \frac{1}{2}\frac{\mu}{a^3}\left[1 - 3\cos(2\lambda) + e\left(\frac{3}{2}\cos(\lambda+\omega)\right.\right. \\
&\quad \left.\left. + 3\cos(\lambda-\omega) - \frac{21}{2}\cos(3\lambda-\omega)\right)\right] \\
&\quad + O(e^2), \\
T_{23} &= 0, \\
T_{33} &= -\frac{\mu}{a^3}[1 + 3e\cos(\lambda-\omega)] + O(e^2).
\end{aligned} \tag{6}$$

If the satellite is not spined (i.e. quasi-inertial pointing), these are also the components in the instrumental frame up to a constant phase. It clearly appears that the main contribution of the EP signal is in the orbital plane at the frequency Λ (spectral line 1 in short) while the components of the gravity gradient in the orbital plane have essentially the frequency 2Λ (spectral line 2). However, it is important to note the $O(e)$ contribution of the gravity gradient to the spectral line 1. This shows that it is necessary to compute some off-centring (thanks to the large signal at spectral line 2) in

order to discriminate the EP contribution. That is why the natural strategy consists in computing some off-centring components using the spectral line 2 and the EP contribution using the spectral line 1. We have to keep in mind that we cannot use the low frequencies (and in particular the 0 frequency) for which the accelerometer measurements are irrelevant.

The situation is slightly different when the satellite is spined around the axes normal to the orbital plane; setting the slowly varying angle ω to 0 (in order to simplify the presented analysis), we have in this case:

$$\begin{aligned} g_1 &= -\frac{\mu}{a^2}[\cos(aep) + 2e\cos(ae\,p+\lambda)] + O(e^2),\\ g_2 &= -\frac{\mu}{a^2}[\sin(aep) + 2e\sin(ae\,p+\lambda)] + O(e^2),\\ g_3 &= 0, \end{aligned} \tag{7}$$

$$\begin{aligned} T_{11} &= \frac{1}{2}\frac{\mu}{a^3}\,[1 + 3\cos(2aep)\\ &\quad + e\left(-\frac{3}{2}\cos(2aep-\lambda)\right.\\ &\quad \left. + \frac{21}{2}\cos(2aep+\lambda) + 3e\cos\lambda\right)] + O(e^2),\\ T_{12} &= \frac{1}{2}\frac{\mu}{a^3}\left[3\sin(2aep) + e\left(-\frac{3}{2}\sin(2aep-\lambda)\right.\right.\\ &\quad \left.\left. + \frac{21}{2}\sin(2aep+\lambda)\right)\right] + O(e^2),\\ T_{13} &= 0,\\ T_{22} &= \frac{1}{2}\frac{\mu}{a^3}\,[1 - 3\cos(2aep)\\ &\quad + e\left(\frac{3}{2}\cos(2aep-\lambda)\right.\\ &\quad \left. - \frac{21}{2}\cos(2aep+\lambda) + 3\cos\lambda\right)] + O(e^2),\\ T_{23} &= 0,\\ T_{33} &= -\frac{\mu}{a^3}[1 + 3e\cos\lambda] + O(e^2), \end{aligned} \tag{8}$$

where $aep = \lambda - s$ (s counted positively in the same sense as the mean anomaly) is the argument of the main signal corresponding to the equivalence principle. The great advantage of this rotation is that the gravity gradient has no longer significant contribution to the EP frequency.

The tensor of inertia [**I**] has essentially constant components in the instrumental frame and will not be analysed more here.

4.2. Constraints on the orbit

From (5) we observe that we have to minimise the semi-major axis to maximise the EP signal which is proportional to **g**. However, the altitude must be sufficiently high to reduce the atmospheric drag. Hence, the most interesting value for the altitude is about 600 km ($g \approx 8.2\ \mathrm{m\,s^{-2}}$) where the forces due to the drag and the solar radiation pressure are nearly equal, but 1500 km ($g \approx 6.4\ \mathrm{m\,s^{-2}}$) is still acceptable. Equations (5) and (7) also show that the sensitive axis of the instrument must lie in the orbital plane.

The eccentricity must be small for two reasons: (i) to concentrate the power spectrum of the EP signal in a unique line (spectral line 1), and (ii) to limit the contribution of the gravity gradient at spectral line 1 when the satellite is not spined. In the MICROSCOPE mission we will be able to recover the in-plane off-centring with an accuracy better than or equal to 10^{-7} m; that is why the eccentricity must be smaller than 10^{-2} to limit the perturbative effects of the gravity gradient in case of null spin. As for the inclination, the main constraints are due to power resources; a helio-synchronous orbit is preferred.

The knowledge of the position of the satellite is necessary to compute the gravity gradient. Given the components Δx_j of the off-centring $\mathbf{C'C''}$ and the errors $\tilde{\Delta}X_k$ on the coordinates of the satellite, the induced error on the estimated differential acceleration due to the gravity gradient is

$$\Delta\Gamma_i = \sum_{j=1}^{3}\sum_{k=1}^{3}\frac{\partial^2 g_i}{\partial x_j\,\partial x_k}\Delta x_j\,\Delta X_k. \tag{9}$$

It happens that these derivatives, when expressed in the instrumental frame, have their main contribution (i.e. terms independent of the eccentricity) at the EP frequency. Spinning the instrument does not reject all these terms at other frequencies. The derivatives have magnitudes of the order of μ/a^4, i.e. a few $10^{-13}\ \mathrm{m^{-1}\,s^{-2}}$ for an altitude of 800 km. For a nominal off-centring of 10^{-5} m, a miss-knowledge ΔX_i of 1 km induces an error of a few 10^{-15} on the acceleration which mimics an EP violation. For MICROSCOPE, a more detailed analysis shows that the requirement is that the miss-knowledge of the satellite position must not exceed 500 m at frequencies 0, Λ and 2Λ in the instrumental frame.

4.3. Constrains on the attitude

We have shown that the sensitive axis must lie in the orbital plane to get the maximum EP signal. Moreover, in case of a small departure from

this plane, the instrument becomes sensitive to the out-of-plane component of the off-centring: in that case, T_{13} and T_{23} have contributions $O(e \sin \varepsilon)$ (ε being the inclination of the instrument) which are at the EP frequency in the case of null spin. The induced acceleration due to the out-of-plane component of the off-centring is then $(\mu/r^3)e \sin(\varepsilon)\Delta x_3 \approx 10^{-13}\varepsilon$ for $\Delta x_3 = 10^{-5}$ m. For $\varepsilon = 10^{-2}$ rad, we get an acceleration of 10^{-15} m s^{-2} just at the limit of what we want to detect but not enough to improve the knowledge of Δx_3. This leads to specify that the angle between the sensitive axis and the orbital plane be smaller than 10^{-2} rad. Let us note that (i) the limit can be relaxed in spined mode, and (ii) this limit depends on the eccentricity of the orbit. A more detailed analysis taking into account the geometric characteristics of the instrument and their stability, evidences other constraints on the stability of the angular velocity and angular acceleration which are summarised in Tables 3 and 4.

The knowledge of the orientation of the instrument is necessary to compute the gravity gradient with a sufficient accuracy. As we require a relative accuracy of 1% on the computation of the off-centring, we need to know the orientation with an accuracy of 10^{-2} rad with respect to the Earth.

5. CONCLUSION

By taking advantage of the micro-satellite product line developed by CNES, the definition of the space MICROSCOPE mission has demonstrated the possibility to perform the EP test with a 10^{-15} accuracy, i.e. quite three orders of magnitude better than the present on ground experiments. The satellite is less than 120 kg, compatible with low-cost launch and the design of the instrument deals with the in orbit conditions of temperature, mass, volume and power. The mission is now selected and the launch is foreseen in 2004. On the basis of the above presented results, the prototype of the instrument will be produced and tested next year, first in the laboratory and then in free fall as envisaged in the specific drop tower of the University of Bremen [23]. In parallel, all the specifications detailed previously which concerns the satellite attitude and motion will be assessed by exploiting the simulation software in development. An important effort needs to be made to detail the experimental procedures of all the mission phases in order to confirm the compatibility of the design of the instrument and the satellite, to implement all the necessary telecommands and telemeasures and to evaluate the accuracy of each envisaged calibration and EP test. Because of the accelerometer's high sensitivity, their resolution cannot be directly verified on ground; thus the in orbit demonstration of the instrument performance is mandatory and dedicated on ground experimental investigations are envisaged to estimate the maximum levels of the error sources.

Acknowledgements—The authors would like to acknowledge the work of the Cnes team in charge of the satellite pre-definition study. The work described in this paper was carried out in part with support from Cnes.

REFERENCES

1. Adelberger, E. G., et al., *Physical Review* D, 1990, **42**, 3267.
2. Su, Y., et al., *Physical Review* D, 1994, **50**, 3614.
3. Baesler, S., et al., Improved test of the equivalence principle for gravitational self energy. *Physical Review Letters*, 1999, **83**(18).
4. Dickey, J. O., et al., *Science*, 1994, **265**, 482.
5. Eddington, A. S., *Mathematical Theory of Relativity*. Cambridge University Press, Cambridge, 1922.
6. Nordtvedt, K., *Astrophysics Journal*, 1993, **407**, 758.
7. Isham, C. J., *Classical and Quantum Gravity*, 1996, **13**, A5–A9.
8. Fayet, P, *Classical and Quantum Gravity*, 1996, **13**, A19–A31.
9. Damour, T. and Polyakov, A. M., *Nuclear Physics* B, 1994, **423**, 532.
10. Bonneville R., GEOSTEP: a gravitation experiment in earth Orbiting Satellite to Test the Equivalence Principle. *Proceedings COSPAR 31*, *Birmingham*, 1995.
11. Worden, P., et al., *Classical and Quantum Gravity*, 1996, **13**, A155–A158.
12. Touboul, P., Rodrigues, M., Willemenot, E. and Bernard, A., Electrostatic accelerometers for the Equivalence Principle test in space. *Classical and Quantum Gravity*, 1996, **13**, A67–A78.
13. Marcuccio, S., Genovese, A., and Andrenucci, M., *FEEP Microthruster Technology Status and Potential Applications*. AIAA, New York, 1997.
14. Fehringer, M., Rüdenauer, F. and Steiger, W., Micronewton indium thrusters. *26th International Electric Propulsion Conference*, *Kitakyushu*, *Japan*, October 17–21, 1999.
15. Reigber, C., et al., CHAMP Phase B Executive Summary, *GFZ*, *STR96/13*, 1996.
16. Web site, (http://op.gfz-potsdam.de/champ/), from launch date 15th July 2000, in orbit conditions and scientific data.
17. GRACE—Gravity Recovery and Climate Experiment: Science and Mission Requirements Document, revision A. *JPL D-15928*, NASA's Earth System Science Pathfinder Program, 1998.
18. Touboul, P., Willemenot, E., Foulon, B. and Josselin, V., Accelerometers for CHAMP, GRACE and GOCE. *Bolletino di Geofisica Teorica Ed Applicata*, bg090, 2000.

19. Gravity Field and Steady State Ocean Circulation Mission. *ESA Publication* SP-1233-1, 1999.
20. Willemenot, E., Pendule de torsion à suspension électrostatique. Thesis, University of Orsay—Paris XI, June 1997.
21. Josselin, V., Architecture mixte pour les accéléromètres ultrasensibles dédiés aux missions spatiales de Physique Fondamentale. Thesis, University of Orsay—Paris XI, October 1999.
22. Danzmann, K., LISA and ground-based detectors for gravitational waves. *Proceedings of the 2nd International Symposium on LISA*, *Pasadena*, *USA*, 1998.
23. Dittus, H., Drop tower Bremen: a weightlessness laboratory on Earth. *Endaveour* (*New Series*), 1991, **15**(2).